JOURNAL OF SOLID STATE CHEMISTRY **131,** 131–137 (1997)
ARTICLE NO. SC977365

Hydrothermal Synthesis and Structures of $Na_3In_2(PO_4)_3$ and $Na_3In_2(AsO_4)_3$: Synthetic Modifications of the Mineral Alluaudite

Kwang-Hwa Lii* and Jinhua Ye†

*Institute of Chemistry, Academia Sinica, Taipei, Taiwan; and †National Research Institute for Metals, 1-2-1 Sengen, Tsukuba, Ibaraki 305, Japan

Received January 21, 1997; accepted February 26, 1997

Two indium-containing analogs of the mineral alluaudite, $Na_3In_2(PO_4)_3$ and $Na_3In_2(AsO_4)_3$, have been synthesized hydrothermally and structurally characterized by single-crystal and powder X-ray diffraction, respectively. Crystal data: $Na_3In_2(PO_4)_3$, $a = 12.450(1)$, $b = 12.786(1)$, $c = 6.5920(7)$ Å, $\beta = 114.174(2)^\circ$, $V = 957.38$ Å^3, $Z = 4$; $Na_3In_2(AsO_4)_3$, as above except $a = 12.6037(2)$, $b = 13.1711(2)$, $c = 6.8342(1)$ Å, $\beta = 113.743(1)^\circ$, $V = 1038.48$ Å^3. The two compounds are isostructural. The main structural feature is the presence of infinite chains of edge-sharing In_2O_{10} dimers and NaO_6 octahedra, which are linked together by PO_4 or AsO_4 tetrahedra to form a framework structure, enclosing two types of tunnels where Na^+ cations reside. The $X(1)$ site of the alluaudite structure is occupied by Na^+, whereas the $X(2)$ site is empty. Instead, a site which is shifted from the $X(2)$ site by $\pm 1/4$ along z is occupied by Na^+.

INTRODUCTION

The phosphate $Na_3Fe_2(PO_4)_3$ adopts the well-known NASICON structure (1–3). In contrast, the corresponding arsenate, $Na_3Fe_2(AsO_4)_3$, exhibits two polymorphs: a low-temperature, garnet-type form and a high-temperature, rhombohedral form (4). The framework of the high-temperature form consists of a tetramer of edge-sharing FeO_6 octahedra. For the arsenates of Group 13 elements $Na_3Al_2(AsO_4)_3$ and $Na_3Ga_2(AsO_4)_3$, the high-temperature form of the iron compound is the only form observed (5, 6). Consequently, it is of interest to know whether the corresponding indium arsenate and phosphate, $Na_3In_2(AsO_4)_3$ and $Na_3In_2(PO_4)_3$, adopt a structure similar to that of the high-temperature form of $Na_3Fe_2(AsO_4)_3$.

Aluminum phosphates have been extensively studied because of their sorption and catalytic properties. Relative to the large number of aluminum and gallium phosphates, there are few indium phosphates in literature, namely, $Li_3In_2(PO_4)_3$ (7), $LiInP_2O_7$ (8), $NaCdIn_2(PO_4)_3$ (9), $[(CH_2NH_3)_2][In_2(HPO_4)_4]$ (10), $Cs[In_2(PO_4)(HPO_4)_2(H_2O)]$ (11), $RbIn(OH)PO_4$ (12), $Na_3In(PO_4)_2$ (13), $KIn(OH)PO_4$ (14), $[In_8(HPO_4)_{14}(H_2O)_6](H_2O)_5(H_3O)(C_3N_2H_5)_3$ (15), and $CaIn_2(PO_4)(HPO_4)$ (16). It is surprising to find that the mineral yanomamite, $InAsO_4 \cdot 2H_2O$ (17), is the only structurally characterized indium arsenate. As part of our continuing study on the structural chemistry of phosphates and arsenates containing mixed octahedral–tetrahedral frameworks, we have also examined the A–In–X–O (A = alkali metals, X = P, As) systems. Recently, we reported $RbIn(OH)PO_4$ which consists of spirals of *cis*-corner sharing InO_6 octahedra (12). In this paper, we report the synthesis and characterization $Na_3In_2(PO_4)_3$ and $Na_3In_2(AsO_4)_3$ whose crystal structures have been determined by single-crystal and powder X-ray diffraction, respectively. Their structures are similar to that of the mineral alluaudite.

EXPERIMENTAL

Synthesis. High-temperature, high-pressure hydrothermal synthesis was performed in gold ampoules contained in a Leco Tem-Pres autoclave where pressure was provided by water pumped by a compressed air driven intensifier. Crystals of $Na_3In_2(PO_4)_3$ were obtained by heating a mixture of 0.5607 g of $Na_2HPO_4 \cdot 2H_2O$, 0.1388 g of In_2O_3, and 0.7 mL of 3 M H_3PO_4 (Na : P mole ratio = 1.2) to 600°C. The autoclave was soaked at this temperature for 36 h, achieving a pressure of 35,000 psi. It was then cooled to 275°C at 5°C/h and quenched to ambient temperature by removing the autoclave from the furnace. The product was filtered off, washed with water, rinsed with methanol, and dried in a desiccator at ambient temperature. The product contained colorless rod crystals of $Na_3In_2(PO_4)_3$ and colorless powder. The X-ray powder pattern of the bulk product could not be indexed based on the structure of $Na_3In_2(PO_4)_3$, indicating that the colorless powder is either a different compound or a mixture.

For the synthesis of $Na_3In_2(AsO_4)_3$, a mixture of 0.5616 g of $Na_2HAsO_4 \cdot 7H_2O$, 0.0833 g of In_2O_3, and 0.4 mL of 3 M H_3AsO_4 (Na : As mole ratio = 1.2) was heated in a gold ampoule under a reaction condition the same as that for

0022-4596/97 $25.00

$Na_3In_2(PO_4)_3$. The product was a colorless microcrystalline powder from which it was possible to completely index the Bragg peaks in the X-ray diffraction pattern. The monoclinic unit cell obtained ($a = 12.6037(2)$, $b = 13.1711(2)$, $c = 6.8342(1)$ Å, $\beta = 113.743(1)^\circ$) and the diffraction pattern itself bore a close resemblance to the calculated pattern of $Na_3In_2(PO_4)_3$. The sample was used for structure analysis by powder X-ray diffraction, as follows.

Single-crystal X-ray diffraction. A colorless crystal of dimensions $0.4 \times 0.07 \times 0.03$ mm was used for indexing and intensity data collection on a Siemens Smart-CCD diffractometer equipped with a normal focus, 3 kW sealed tube X-ray source. Intensity data were collected in 2300 frames with increasing ω (width of 0.3° per frame). The orientation matrix and unit cell parameters were determined by a least-squares fit of 1905 reflections with $6^\circ < 2\theta < 40^\circ$. Of the 2236 reflections collected ($2\theta_{max} = 53.5^\circ$), 847 unique reflections were considered observed ($I > 2.5\sigma(I)$) after Lp and empirical absorption corrections ($R_{int} = 0.025$). Correction for absorption was based 1936 reflections using the SHELXTL PC program package ($T_{min/max} = 0.654/0.983$) (18). On the basis of systematic absences, statistical analysis of the intensity distribution, and successful solution and refinement of the structure, the space group was determined to be $C2/c$. The structure was solved by direct methods and successive Fourier synthesis, and was refined by full-matrix least-squares refinement based on F values. The Na atoms and P(2) are at special positions, and all other atoms are at general positions. The occupancy factor of each metal atom was allowed to refine but in no case deviated significantly from full occupancy. The final cycle of full-matrix least-squares refinement including atomic coordinates and anisotropic thermal parameters converged at $R = 0.0173$ and $R_w = 0.0214$. The final difference electron density map was featureless and the highest peak and deepest hole were 0.50 and -0.47 e/Å^3, respectively. Neutral-atom scattering factors for all atoms were used. Anomalous dispersion and secondary extinction corrections were applied. Structure solution and refinement were performed on a VAX computer system using SHELXTL-Plus programs.

Powder X-ray diffraction. Powder X-ray diffraction data of $Na_3In_2(AsO_4)_3$ were recorded on a Rigaku RINT-2000 diffractometer with graphite monochromatized Cu$K\alpha$ radiation. The data were collected with a step scan procedure in the range of $2\theta = 5^\circ$ to 100°. The step interval was 0.024° and scan speed, 1° min^{-1}. Structure refinement was carried out using the Rietveld program RIETAN (19) based on the structure model of $Na_3In_2(PO_4)_3$ determined from the X-ray single crystal structure analysis. Positional parameters and isotropic thermal parameters of all atoms were refined. The other variable parameters were an overall scale factor, background parameters, FWHM parameters, an asymmetry parameter determining the shape of the Bragg peaks, a zero point for the Bragg angles, and a preferred-orientation parameter. The final cycle of refinement converged to $R_F = 0.0158$ and $R_I = 0.0273$, indicating good agreement between the observed and calculated intensities. The final Rietveld fit is shown in Fig. 1.

Table of anisotropic thermal properties for $Na_3In_2(PO_4)_3$ is submitted as supplementary materials.

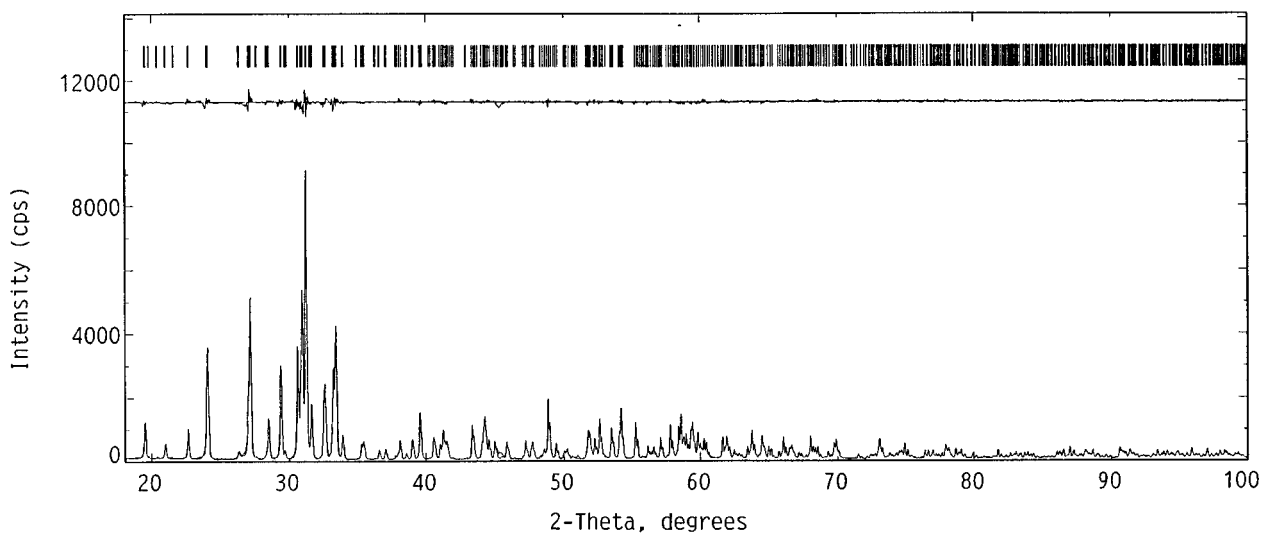

FIG. 1. Final Rietveld profile fit (1.54178 Å) of the laboratory X-ray powder data collected on $Na_3In_2(AsO_4)_3$ over the range $2\theta = 18$–100°, with experimental data (bottom), a difference plot (middle), and positions of Bragg reflections (top).

RESULTS AND DISCUSSION

The crystallographic data are listed in Table 1, atomic coordinates in Table 2, and interatomic distances, bond angles, and bond-valence sums (20) in Table 3. Atoms Na(1), Na(2), and P(2) (or As(2)) sit on 2-fold axes, Na(3) has a local symmetry of $\bar{1}$, and all other atoms are at general positions. The In and P (or As) atoms are six- and four-coordinated, respectively. The bond-valence sum for Na(2) indicates that it is loosely bound.

The alluaudite structure type has the general formula $X(2)X(1)M(1)M(2)_2(PO_4)_3$, in which $X(2)$ and $X(1)$ are large unipositive or dipositive cation sites and $M(1)$ and $M(2)$ are occupied by some distribution of Mn^{2+}, Fe^{2+}, or Fe^{3+} (21, 22). For the unoxidized end member the composition is $NaCaMn^{2+}Fe_2^{2+}(PO_4)_3$. The structure appears to be highly susceptible to partial oxidation. However, an example of unoxidized variant, $NaMn_3^{2+}(PO_4)(HPO_4)_2$, was synthesized under reducing hydrothermal conditions (23). On the other hand, the oxidized end member, $NaMn^{2+}Fe_2^{3+}(PO_4)_3$, did not proceed to the completely oxidized equivalent $Mn^{3+}Fe_2^{3+}(PO_4)_3$. The crystal structure of alluaudite consists of infinite chains of edge-sharing $M(1)O_6$ and $M(2)O_6$ polyhedra, which are linked by phosphate tetrahedra to form sheets. Symmetry-equivalent sheets are held together by phosphate oxygens to form a three-dimensional architecture with two sets of tunnels at 1/2, 0, z and 0, 0, z. Crystal structure analysis of a natural alluaudite from the Buranga pegmatite of Central Africa indicates that the $X(1)$ site (at 1/2, 0, 0) is partly filled with Na^{2+}, Ca^{2+}, and Mn^{2+}, and the $X(2)$ site (at 0, 0, 0) is empty.

Figure 2 shows a polyhedral representation of the $Na_3In_2(PO_4)_3$ structure viewed along the [001] direction. A slice of the structure parallel to the (010) plane is shown in Fig. 3. The structure is closely related to the alluaudite structure type, but there are a number of important differences. In $Na_3In_2(PO_4)_3$, the $X(1)$ site (at 1/2, 0, 0) is

TABLE 1
Crystallographic Data for $Na_3In_2(PO_4)_3$ and $Na_3In_2(AsO_4)_3$

Formula	$Na_3In_2(PO_4)_3$	$Na_3In_2(AsO_4)_3$
M	583.52	715.37
Crystal system	monoclinic	monoclinic
Space group	$C2/c$	$C2/c$
a(Å)	12.450(1)	12.6037(2)
b(Å)	12.786(1)	13.1711(2)
c(Å)	6.5920(7)	6.8342(1)
β(°)	114.174(2)	113.743(1)
V(Å)	957.4	1038.48
Z	4	4
D_c (g cm^{-1})	4.048	4.576
F(000)	1088	1304
μ (cm^{-1})	55.3 (Mo$K\alpha$)	48.1 (Cu$K\alpha$)
T (°C)	23	23
λ (Å)	0.71073	1.54178
Maximum 2θ(°)	53.5	100
Reflection collected	2236	
Unique reflections	894	
Obsd unique reflns ($I > 2.5\sigma(I)$)	847	1084
$T_{min/max}$	0.654/0.983	
Weighting scheme	$w^{-1} = \sigma^2(F) + 0.000457F^2$	
Number of parameters	95	83
R_F[a]	0.0173	0.0158
R_w[b]	0.0214	
Goodness-of-fit	1.14	
$(\Delta\rho)_{max}$; $(\Delta\rho)_{min}$ (e Å^{-3})	0.50; −0.47	
R_I[c]		0.0273
R_{wp}[d]		0.0987
R_p[e]		0.0686
R_e[f]		0.0552

[a] $R = \sum||F_o| - |F_c||/\sum|F_o|$.
[b] $R_w = [\sum w(|F_o| - |F_c|)^2/\sum w|F_o|^2]^{1/2}$.
[c] $R_I = \sum|I_o - I_c|/\sum I_o$.
[d] $R_{wp} = [\sum w_i(y_{oi} - y_{ci})^2/\sum w_i y_{oi}^2]^{1/2}$.
[e] $R_p = \sum|y_{oi} - y_{ci}|/\sum|y_{oi}|$.
[f] $R_e = [(N_p - N_r - N_c)/\sum w_i y_{oi}^2]^{1/2}$.

TABLE 2
Atomic Coordinates and Thermal Parameters for $Na_3In_2(PO_4)_3$ and $Na_3In_2(AsO_4)_3$

	$Na_3In_2(PO_4)_3$			
Atom	x	y	z	U_{eq}[a] (Å$^2 \times 100$)
Na(1)	0	0.2767(2)	0.25	1.68(8)
Na(2)	0	0.0071(2)	0.75	3.1(1)
Na(3)	0.5	0	0.5	2.03(8)
In	0.22774(2)	0.15589(2)	0.15504(4)	0.77(2)
P(1)	0.23934(7)	−0.10171(7)	0.1347(1)	0.75(3)
P(2)	0	0.2732(1)	0.75	0.72(4)
O(1)	0.3635(2)	−0.0766(2)	0.1692(4)	1.48(9)
O(2)	0.2377(2)	−0.1709(2)	0.3299(4)	0.98(9)
O(3)	0.1660(2)	−0.0015(2)	0.1239(4)	0.97(9)
O(4)	0.1712(2)	−0.1624(2)	−0.0848(5)	1.1(1)
O(5)	0.0516(2)	0.2028(2)	0.9568(4)	1.17(9)
O(6)	0.0890(2)	0.3474(2)	0.7173(5)	1.1(1)
	$Na_3In_2(AsO_4)_3$			
Atom	x	y	z	B^b (Å^2)
Na(1)	0	0.276(1)	0.25	0.9(5)
Na(2)	0	−0.002(1)	0.75	3.9(6)
Na(3)	0.5	0	0.5	1.8(5)
In	0.2228(2)	0.1563(2)	0.1456(5)	0.63(6)
As(1)	0.2388(4)	−0.1039(3)	0.1324(7)	0.7(1)
As(2)	0	0.2766(4)	0.75	0.8(1)
O(1)	0.372(2)	−0.079(2)	0.180(3)	1.7(6)
O(2)	0.230(1)	−0.176(1)	0.336(3)	−0.4(4)
O(3)	0.158(2)	0.002(1)	0.122(3)	1.9(5)
O(4)	0.168(2)	−0.165(2)	−0.109(3)	1.8(6)
O(5)	0.044(2)	0.202(1)	0.973(3)	0.2(5)
O(6)	0.094(2)	0.360(1)	0.716(3)	0.4(5)

[a] U_{eq} is defined as one-third of the trace of the orthogonalized U_{ij} tensor.
[b] All atoms of $Na_3In_2(AsO_4)_3$ is refined with isotropic thermal parameters.

TABLE 3
Interatomic Distances and Bond Valence Sums ($\sum$s) for $Na_3In_2(PO_4)_3$ and $Na_3In_2(AsO_4)_3$

$Na_3In_2(PO_4)_3$

The InO_6 octahedron[a]

In	O(2a)	O(2b)	O(3)	O(4)	O(5)	O(6)
O(2a)	**2.250(2)**	2.941(5)		3.153(4)	2.906(3)	2.819(3)
O(2b)	82.6(1)	**2.206(3)**	3.291(4)		2.797(5)	2.889(3)
O(3)	170.8(1)	98.6(1)	**2.134(2)**	2.825(4)	2.964(3)	3.416(4)
O(4)	92.7(1)	163.5(1)	83.6(1)	**2.105(4)**	2.816(4)	3.440(4)
O(5)	83.1(1)	80.4(1)	88.1(1)	83.4(1)	**2.129(2)**	
O(6)	81.0(1)	84.6(1)	108.1(1)	110.4(1)	159.4(1)	**2.084(3)**

$\sum$s(In–O) = 3.10

The $P(1)O_4$ tetrahedron

P(1)	O(1)	O(2)	O(3)	O(4)
O(1)	**1.502(3)**	2.527(4)	2.540(4)	2.541(3)
O(2)	110.8(1)	**1.569(3)**	2.518(3)	2.513(4)
O(3)	112.2(1)	107.3(2)	**1.558(2)**	2.490(4)
O(4)	112.6(2)	107.3(1)	106.4(1)	**1.552(3)**

$\sum$s(P(1)–O) = 4.87

The $P(2)O_4$ tetrahedron

P(2)	O(5)	O(6)	O(5a)	O(6a)
O(5)	**1.537(3)**	2.594(4)	2.493(5)	2.480(3)
O(6)	115.0(1)	**1.540(3)**	2.480(3)	2.425(7)
O(5a)	108.4(2)	107.4(2)	**1.537(3)**	2.493(5)
O(6a)	107.4(2)	103.9(2)	115.0(1)	**1.540(3)**

$\sum$s(P(2)–O) = 4.94

Na(1)–O(1)	2.439(3) (2×)	Na(1)–O(4)	2.442(3) (2×)
Na(1)–O(5)	2.461(3) (2×)		

$\sum$s(Na(1)–O) = 1.05

Na(2)–O(3)	2.487(3) (2×)	Na(2)–O(3)	2.525(3) (2×)
Na(2)–O(4)	2.919(3) (2×)	Na(2)–O(5)	2.795(4) (2×)

$\sum$s(Na(2)–O) = 0.83

Na(3)–O(1)	2.359(2) (2×)	Na(3)–O(1)	2.578(3) (2×)
Na(3)–O(6)	2.405(2) (2×)		

$\sum$s(Na(3)–O) = 1.08

$Na_3In_2(AsO_4)_3$

The InO_6 octahedron[a]

In	O(2a)	O(2b)	O(3)	O(4)	O(5)	O(6)
O(2a)	**2.27(2)**	2.86(4)		3.16(3)	3.06(2)	2.88(3)
O(2b)	79.9(7)	**2.17(2)**	3.38(3)		2.87(3)	3.01(2)
O(3)	173.4(8)	101.8(7)	**2.18(2)**	2.80(3)	2.98(3)	3.40(3)
O(4)	93.6(8)	161.5(7)	82.8(9)	**2.05(3)**	2.69(3)	3.37(3)
O(5)	87.2(7)	82.9(8)	86.7(7)	79.4(8)	**2.16(2)**	
O(6)	81.9(6)	88.8(7)	104.4(7)	107.6(8)	167.4(8)	**2.12(2)**

$\sum$s(In–O) = 3.04

The $As(1)O_4$ tetrahedron

As(1)	O(1)	O(2)	O(3)	O(4)
O(1)	**1.61(2)**	2.74(3)	2.77(3)	2.77(3)
O(2)	110.5(9)	**1.72(2)**	2.72(3)	2.82(3)
O(3)	113 (1)	105 (1)	**1.71(2)**	2.74(3)
O(4)	112 (1)	110 (1)	105.8(9)	**1.73(2)**

$\sum$s(As(1)–O) = 4.93

TABLE 3—*Continued*

		The $As(2)O_4$ tetrahedron			
As(2)	O(5)	O(6)	O(5a)	O(6a)	
O(5)	**1.71(1)**	2.94(3)	2.79(4)	2.69(3)	
O(6)	119.8(8)	**1.72(2)**	2.69(3)	2.60(5)	
O(5a)	109 (1)	104 (1)	**1.71(2)**	2.94(3)	
O(6a)	104 (1)	100 (1)	119.8(8)	**1.70(2)**	
$\sum s(As(2)–O) = 4.77$					
Na(1)–O(1)	2.42(3) (2 ×)		Na(1)–O(4)		2.43(3) (2 ×)
Na(1)–O(5)	2.39(2) (2 ×)				
$\sum s(Na(1)–O) = 1.14$					
Na(2)–O(3)	2.47(3) (2 ×)		Na(2)–O(3)		2.52(2) (2 ×)
Na(2)–O(4)	2.90(3) (2 ×)		Na(2)–O(5)		3.02(3) (2 ×)
$\sum s(Na(2)–O) = 0.79$					
Na(3)–O(1)	2.37(2) (2 ×)		Na(3)–O(1)		2.60(3) (2 ×)
Na(3)–O(6)	2.37(2) (2 ×)				
$\sum s(Na(3)–O) = 1.10$					

[a]The distances between *trans* oxygen atoms are not shown.

occupied by Na(3), whereas the $X(2)$ site (at 0, 0, 0) is empty. Instead, a site in the tunnel at 0, 0, z shifted from the $X(2)$ site by $\pm 1/4$ along z is occupied by Na(2), which is similar to that observed in $NaCo_3(PO_4)(HPO_4)_2$ (24) and $NaMn_3(PO_4)(HPO_4)_2$ (25). The $X(2)$ site in $Na_3In_2(PO_4)_3$ is so distorted, with two extremely short distances (1.886 Å), that there is no possibility for a Na^+ cation to reside. The $M(1)$ site is occupied by Na(1) and the $M(2)$ site by In such that the infinite chains of $M(1)$–$M(2)$–$M(2)$ triplets consist of dimers of edge-sharing InO_6 octahedra which are separated by $Na(1)O_6$ octahedra. These infinite chains are linked together by $P(1)O_4$ and $P(2)O_4$ tetrahedra to form sheets in the (010) plane, which are further connected by

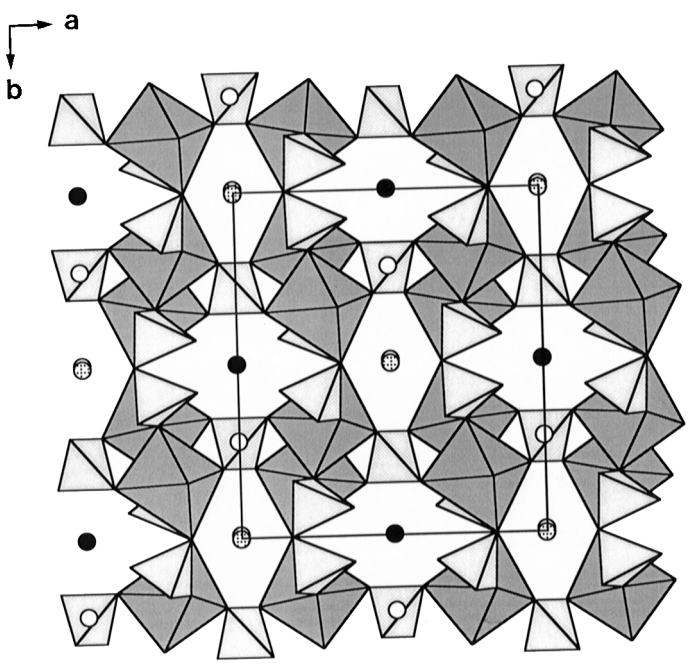

FIG. 2. Structure of $Na_3In_2(PO_4)_3$ as viewed along the [001] direction. In this presentation, the corners of octahedra and tetrahedra are oxygen atoms and the indium and phosphorus are at the center of each octahedron and tetrahedron, respectively. Open circles, Na(1); stippled circles, Na(2); solid circles, Na(3).

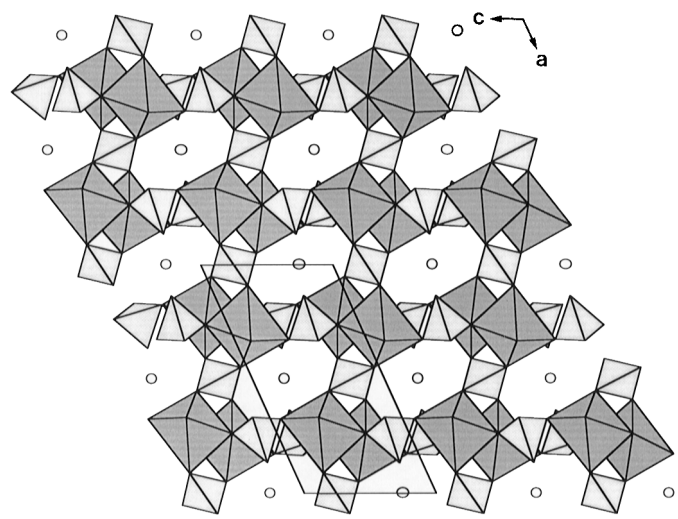

FIG. 3. Slice of the $Na_3In_2(PO_4)_3$ structure parallel to the (010) plane showing the In_2O_{10} dimers. Open circles are Na(1) atoms. The other Na atoms are not shown for clarity.

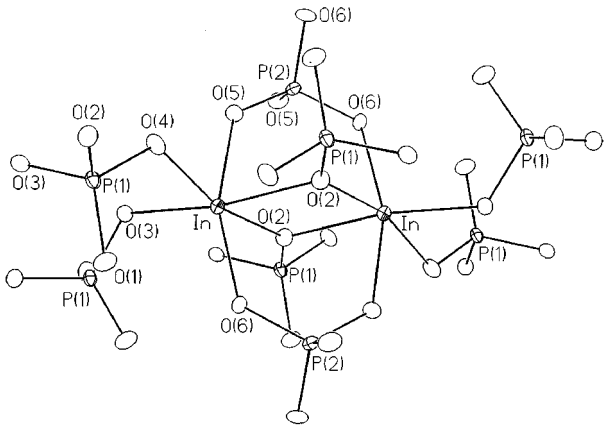

FIG. 4. The coordination of phosphate ligands around a dimer of edge-sharing InO_6 octahedra in $Na_3In_2(PO_4)_3$.

$P(2)O_4$ tetrahedra to form the three-dimensional framework structure.

In $Na_3In_2(PO_4)_3$, two InO_6 octahedra sharing a common edge form a unit In_2O_{10}, which has a point group symmetry of C_i (Fig. 4). The ten vertices of the dimer are shared with eight PO_4 tetrahedra. Two of the eight phosphates form bridges between two In atoms in a dimer. As shown by the O ··· O distances 2.797–3.440 Å, the InO_6 octahedron is highly distorted. The length of the shared edge is 2.941 Å. The indium atoms are displaced from the centroids of their InO_6 octahedra away from each other such that the In ··· In separation is increased from 3.00 to 3.35 Å. The strong distortion in InO_6 probably results from the need to accommodate to the connectivity of the PO_4 tetrahedra, which are rather rigid entities and are responsible for holding neighboring dimers together. The average P–O distances (P(1)–O, 1.545 Å; P(2)–O, 1.538 Å) are consistent with those typically observed in phosphates. Atom P(2) sits on a 2-fold axis and has a more symmetric neighborhood than P(1). The P(1)–O(1) bond length (1.502 Å) is the shortest because O(1) is only coordinated to Na atoms.

The coordination number of each Na atom was determined on the basis of the maximum gap in the Na–O distances ranked in increasing order. The maximum cation–anion distance for Na–O, 3.19 Å, according to Donnay and Allmann (26), was also considered. The inner coordination environment of Na(1) is a strongly distorted octahedron as indicated by the O ··· O distances 2.816–4.253 Å and the angle 134.9° subtended by two of the axial oxygen atoms. There are two neighboring oxygens, O(6), at a distance of 2.956 Å. The coordination polyhedron approximates a bicapped octahedron with two of the octahedral edges being capped by oxygen atoms. The coordination polyhedron of Na(2) is also highly irregular and consists of an inner coordination shell of four oxygen atoms at distances of 2.487 and 2.525 Å, and an outer shell of four oxygens at 2.795 and 2.919 Å. The inner coordination environment of Na(2) is roughly square planar in the (101) plane, with fairly regular Na–O bond lengths. The four outer oxygen atoms are loosely bound, which can be correlated to the markedly anisotropic thermal ellipsoid of Na(2) ($U_{22} \approx 3U_{11} \approx 3U_{33}$). The $Na(3)O_6$ octahedron, as indicated by the Na(3)–O distances 2.359–2.578 Å and the O ··· O distances 3.003–3.980 Å, is considerably more regular.

The mineral caryinite, an arsenate containing Mn, Mg, Ca, Pb, and Na, has been suggested to belong to the alluaudite structure type (22). To our knowledge, the crystal structure of caryinite has not yet been reported. There are few structurally characterized arsenates with the alluaudite structure in literature. A pure cobalt-containing variant of alluaudite, $NaCo_3(AsO_4)(HAsO_4)_2$, has been synthesized hydrothermally and characterized by single-crystal X-ray diffraction. The high-temperature polymorphs of the garnet arsenates $NaCa_2M_2(AsO_4)_3$ (M = Mg, Co, Ni), as indicated from X-ray powder diffraction, has an alluaudite-like structure. In the present work, the Rietveld structure refinement of the X-ray powder diffraction data of $Na_3In_2(AsO_4)_3$ shows that it is isostructural with $Na_3In_2(PO_4)_3$. The covalent framework and the Na^+ cation sites are essentially the same in both cases. The compound $Na_3In_2(AsO_4)_3$ is another example of arsenate with the alluaudite structure.

In conclusion, an indium phosphate and the corresponding arsenate, $Na_3In_2(PO_4)_3$ and $Na_3In_2(AsO_4)_3$, have been synthesized hydrothermally and structurally characterized. In contrast to $Na_3Al_2(AsO_4)_3$ and $Na_3Ga_2(AsO_4)_3$, which have a structure similar to that of the high-temperature form of $Na_3Fe_2(AsO_4)_3$, the two indium compounds adopt the alluaudite structure type. The main structural feature is the presence of infinite chains of edge-sharing In_2O_{10} dimers and NaO_6 octahedra. The two compounds are not isotypic, strictly speaking, to that of the parent alluaudite, because one of the cation sites is completely different.

ACKNOWLEDGMENTS

Support for this study by the National Science Council (NSC86-2113-M-001-014) is acknowledged. The authors thank Professor S.-L. Wang at National Tsing Hua University for single-crystal X-ray data collection.

REFERENCES

1. F. d'Yvoire, M. Pintard-Screpel, E. Bretey, and M. de La Rochere, *Solid State Ionics* **9–10,** 851 (1983).
2. M. de la Rochere, F. d'Yvoire, G. Collin, R. Comes, and J.-P. Boilot, *Solid State Ionics* **9–10,** 825 (1983).
3. C. Delmas, J.-C. Viala, R. Olazcuaga, G. Le Flem, P. Hagenmuller, F. Cherkaoui, and R. Brochu, *Solid State Ionics* **3–4,** 209 (1981).
4. F. d'Yvoire, M. Pintard-Screpel, and E. Bretey, *Solid State Ionics* **18–19,** 502 (1986).

5. F. d'Yvoire, E. Bretey, and G. Collin, *Solid State Ionics* **28–30,** 1259 (1988).
6. C. Masquelier, F. d'Yvoire, and G. Collin, *J. Solid State Chem.* **118,** 33 (1995).
7. E. A. Genkina, L. A. Muradyan, B. A. Maximov, B. V. Merinov, and S. E. Sigarev, *Kristallografiya* **32,** 74 (1987).
8. T. Q. Duc, S. Hamdoune, and Y. Le Page, *Acta Crystallogr. Sect. C* **43,** 201 (1987).
9. D. Antenucci, G. Miehe, P. Tarte, W. W. Schmahl, and A.-M. Fransolet, *Eur. J. Mineral.* **5**, 207 (1993).
10. S. S. Dhingra and R. C. Haushalter, *J. Chem. Soc., Chem. Commun.* 1665 (1993).
11. S. S. Dhingra and R. C. Haushalter, *J. Solid State Chem.* **112,** 96 (1994).
12. K.-H. Lii, *J. Chem. Soc. Dalton Trans.* 815 (1996).
13. K.-H. Lii, *Eur. J. Solid State Inorg. Chem.* **33,** 519 (1996).
14. J. A. Hriljac, C. P. Grey, A. K. Cheetham, P. D. VerNooy, and C. C. Torardi, *J Solid State Chem.* **123,** 243 (1996).
15. A. M. Chippindale, S. J. Brech, A. R. Cowley, and W. M. Simpson, *Chem. Mater.* **8,** 2259 (1996).
16. X. Tang and A. Lachgar, *Z. Anorg. Allg. Chem.* **622,** 513 (1996).
17. N. F. Botelho, G. Roger, F. d'Yvoire, Y. Moelo, and M. Volfinger, *Eur. J. Mineral.* **6,** 245 (1994).
18. G. M. Sheldrick, "SHELXTL PC, Version 5, "Siemens Analytical X-Ray Instruments, Inc., Madison, WI, 1995.
19. F. Izumi, *J. Crystallogr. Assoc. Jpn.* **27,** 23 (1985).
20. I. D. Brown and D. Altermatt, *Acta Crystallogr. Sect. B* **41,** 244 (1984).
21. D. J. Fisher, *Am. Mineral.* **40,** 1100 (1955).
22. P. B. Moore, *Am. Mineral.* **56,** 1955 (1971).
23. F. Leroux, A. Mar, C. Payen, D. Guyomard, A. Verbaere, and Y. Piffard, *J. Solid State Chem.* **115,** 240 (1995).
24. K.-H. Lii and P.-F. Shih, *Inorg. Chem.* **33,** 3028 (1994).
25. S. Khorari, A. Rulmont, R. Cahay, and P. Tarte, *J. Solid State Chem.* **118, 267** (1995).
26. G. Donnay and R. Allmann, *Am. Mineral.* **55,** 1003 (1970).